



HAL
open science

Influence of excitation pulse length on a correlated two-electron wave packet

M A Lysaght, H W van Der Hart

► **To cite this version:**

M A Lysaght, H W van Der Hart. Influence of excitation pulse length on a correlated two-electron wave packet. *Journal of Physics B: Atomic, Molecular and Optical Physics*, 2010, 43 (12), pp.121001. 10.1088/0953-4075/43/12/121001 . hal-00630003

HAL Id: hal-00630003

<https://hal.science/hal-00630003>

Submitted on 7 Oct 2011

HAL is a multi-disciplinary open access archive for the deposit and dissemination of scientific research documents, whether they are published or not. The documents may come from teaching and research institutions in France or abroad, or from public or private research centers.

L'archive ouverte pluridisciplinaire **HAL**, est destinée au dépôt et à la diffusion de documents scientifiques de niveau recherche, publiés ou non, émanant des établissements d'enseignement et de recherche français ou étrangers, des laboratoires publics ou privés.

Influence of Excitation Pulse Length on a Correlated Two-Electron Wave-Packet

M. A. Lysaght and H. W. van der Hart

Centre for Theoretical Atomic, Molecular and Optical Physics, Queen's University
Belfast, Belfast BT7 1NN, UK

E-mail: m.lysaght@qub.ac.uk

Abstract. We employ the time-dependent R-matrix approach to investigate how ultrafast dynamics in the excited $2s2p^2$ configuration of C^+ is affected by the length of the excitation pulse. The excitation pulse is tuned closer to the 2D state than to the 2S state. We demonstrate that by varying the excitation pulse length, we can choose an excitation of the $2s2p^2$ configuration which is dominated by the 2D state or an excitation which is dominated by a breathing motion between the uncoupled $|2p_02p_0\rangle$ state and the singlet $|2p_{-1}2p_1\rangle$ states.

PACS numbers: 31.14.A-, 32.80.Qk, 32.80.Rm

1. Introduction

One of the main challenges in physics is the development of understanding of the evolution of correlated dynamics within complex systems. The clearest way in which such correlated motion manifests itself within atomic physics is through the core excitation of atoms and molecules leading to collective electron dynamics that typically unfolds on the attosecond time scale [1, 2]. Insight into the basic forms of correlated electron motion forms a prerequisite for the development of schemes to control the motion of electrons in more complex systems ranging from large biomolecules [3] to metallic nanostructures [4].

The recent emergence of attosecond light sources [5] now allows direct time-domain access to ultrafast electron dynamics in atoms [6], molecules [2] and condensed matter systems [7]. As such, attosecond technology not only provides a means of observing, or even controlling, the motion of single electrons, but also affords the promise of providing deeper insight into ultrafast *correlated* dynamics *between* electrons in complex matter. For example, a recent investigation [8] proposed using an attosecond light pulse to doubly ionize a superposition of low-lying doubly excited states in He. By measuring the momentum vectors of the two ejected electrons in coincidence, it would be possible to observe the time-varying collective behaviour of the two electrons.

Although some success has been achieved in understanding the correlated motion of electrons in the time-domain [8, 9], to our knowledge, the possibility of selecting

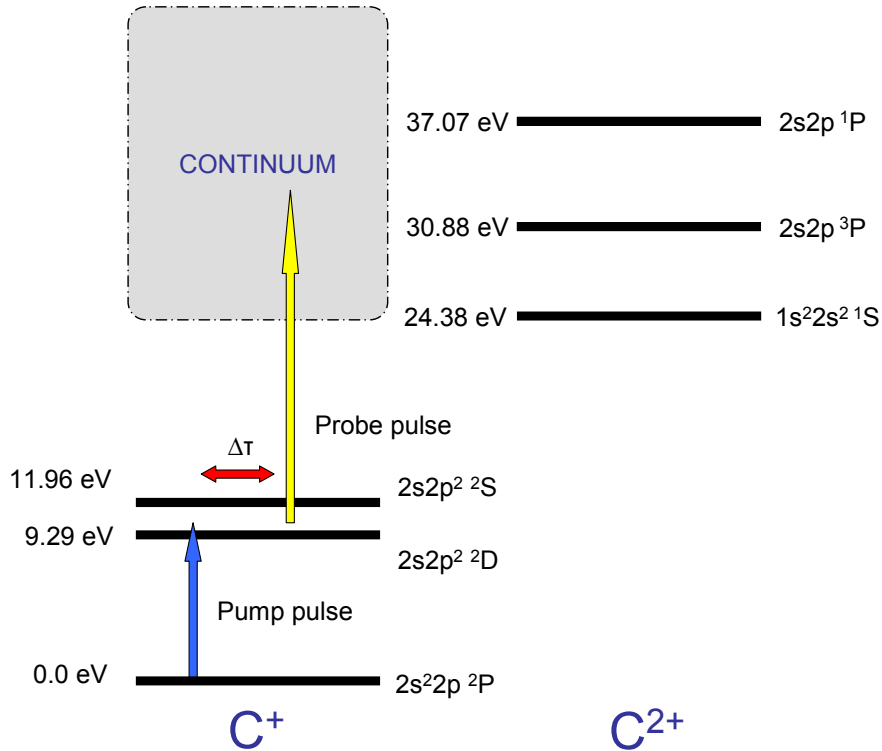


Figure 1. (Color online). Diagram of the pump-probe scheme. The pump pulse coherently populates a superposition of the $2s2p^2\ ^2D$ and 2S states. The time-delayed probe pulse has a central photon energy that allows the transfer of population above the $C^{2+}\ 2s2p\ ^3P$ ionization threshold.

correlated electron dynamics has received little attention. In this report we propose an ultrafast scheme in which we are able to choose the nature of the correlated dynamics occurring between two electrons. We explain the induced ultrafast dynamics and show that by choosing light field parameters carefully, it is possible to steer a multielectron wave-packet into a specific field-free evolution.

2. The pump-probe scheme

Our scheme is similar to a pump-probe scheme used in a previous study of collective electron dynamics in C^+ [9, 10]. The basic features of the scheme are explained in figure 1. We consider a C^+ ion in its $2s^22p\ ^2P^o$ ground state with total magnetic quantum number $M=0$. This ion is excited by an extreme ultraviolet (XUV) pulse, linearly polarized in the z direction, into a superposition of the $2s2p^2\ ^2S^e$ and $^2D^e$ excited states. The energy separation between these two states, caused by the Coulomb repulsion between the two equivalent $2p$ electrons, results in a temporal interference between the two states with a frequency determined by the energy separation. The fact that configurations in an ion are more separated in energy than in a neutral system provides the opportunity to investigate electron-electron dynamics within a single configuration. This is not the case for neutral systems where configurations lie

close in energy with the consequence that inter-configuration interactions will lead to more complicated dielectronic repulsion dynamics [8]. In this naive single-configuration picture, the responsible dielectronic repulsion integral is the $F^2(2p,2p)$ integral [11]. Hence, this repulsion governs the dynamical behaviour of the multielectron wave-packet which continues to evolve after the end of the pump pulse. Subsequent irradiation of the C^+ ion with a time-delayed ultrashort XUV pulse results in ionization. It was found in a previous study that by varying the time-delay between the pump pulse and the ultrashort ionising probe pulse the ionisation probability of the coherent superposition of the $2s2p^2\ ^2D$ and 2S states showed rapid modulation due to collective dynamics of the two equivalent 2p electrons [9]. Ejected electron momentum distributions demonstrated clearly that the oscillations could be ascribed to a breathing motion between two different angular distributions, explaining the modulation of the ionisation yield [10].

In the present study, we aim to investigate the role of electron-electron interactions in the transition from ultrafast excitation to long-pulse excitation. In long-pulse excitation (and the non-relativistic limit), transitions take place between LS-coupled states. In short-pulse excitation, the electrons have little time to adjust to the changes in, for example, angular-momentum couplings between the initial and the final state that occur in LS-coupling. For example, the $M=0$ level of an sp configuration can only be formed from electrons with $m=0$, whereas the $M=0$ levels of a p^2 configuration can be formed either by two $m=0$ electron or by two $|m|=1$ electrons. As a consequence short-pulse excitations can lead to dynamics governed by electron-electron interactions [10]. In this study, we investigate how the transition from short to long excitation pulses affects the dynamics in the $2s2p^2$ configuration of C^+ .

The present investigations are carried out using the recently developed time-dependent R-matrix (TDRM) approach [12, 13]. This approach enables the response of multielectron atoms to ultrashort light fields to be determined from first principles. In it, the solution of the time-dependent Schrödinger equation is accomplished by the standard partitioning of space into an internal and an external region [14]. In the internal region, exchange interactions involving the ejected electron and the residual electrons are important, while these interactions are negligible in the external region. Hence, in the latter region, the ejected electron moves in the local long-range potential of the residual ion together with the laser field. A detailed description of the theory can be found in Ref.[13].

As already mentioned, the pump-probe scheme studied is shown in figure 1, but the details differ slightly from the previous studies. The initial state remains the $M=0$ level of the C^+ ground state. The pump pulse now has a central photon energy $\omega_1 = 10.0$ eV in order to be near-resonant with the $2s2p^2\ ^2S^e$ and $^2D^e$ states but with different detunings. It is defined by a three-cycle \sin^2 ramp-on of the electric field followed by q cycles of constant intensity and finally by a three-cycle \sin^2 ramp-off, giving a total of $n = 6+q$ cycles of the electric field. After letting the pumped C^+ ion freely evolve for ~ 1 fs, we probe the ion by irradiating it with a probe pulse. The probe pulse has a central photon energy $\omega_2 = 21.8$ eV and is described by a three-cycle \sin^2 ramp-on followed

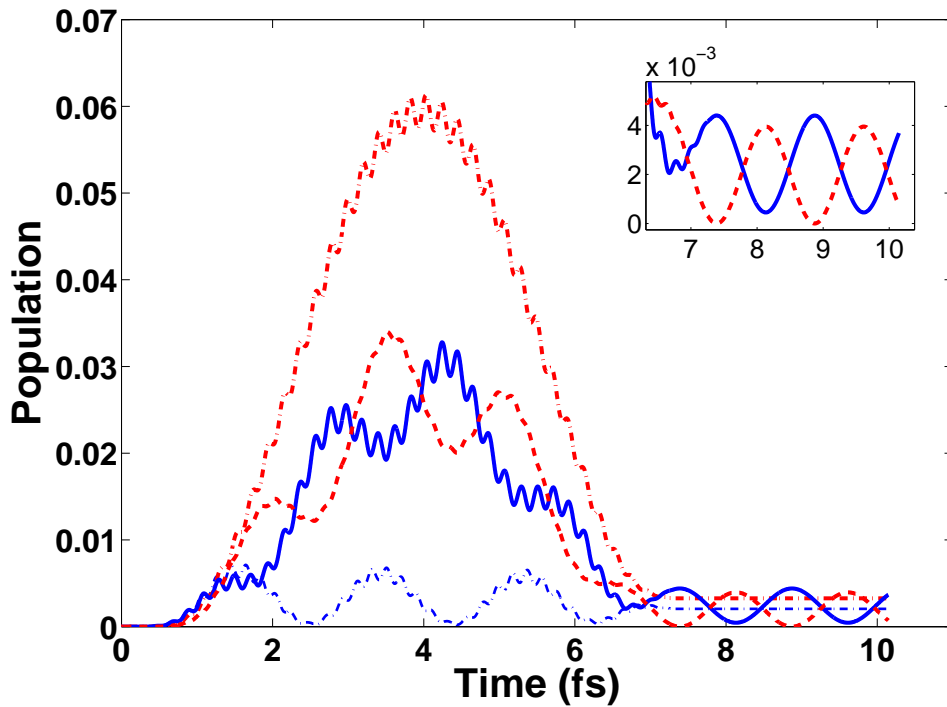


Figure 2. (Color online). Population of the excited $2s2p^2$ bound states as a function of time during and after an 18 cycle (7.5 fs) pump pulse. Populations are given for the LS -coupled 2S state (thin blue dash-dot) and the 2D state (red dash-dot), as well as for the uncoupled $|2p_0,2p_0\rangle$ states (solid blue) and $|2p_1,2p_{-1}\rangle_S$ states (red dash). No probe pulse is present here to show the free evolution of C^+ after the pump pulse. The inset shows the free evolution of the $|2p_0,2p_0\rangle$ and $|2p_1,2p_{-1}\rangle_S$ populations.

by a three-cycle \sin^2 ramp-off of the electric field. This pulse duration remains fixed throughout the study. Both pulses have a maximum intensity of $5 \times 10^{12} \text{ W/cm}^2$. The probe pulse is sufficiently energetic to transfer the population from the $2s2p^2$ ${}^2S^e$ and ${}^2D^e$ excited states to continuum channels coupled to the first excited state of C^{2+} , $2s2p$ ${}^3P^o$. After the probe pulse we allow the system to relax freely for ~ 30 fs. We analyse the dynamics through the angular distributions of the emitted electrons [10]. We thus focus on the channels associated with the $2s2p$ ${}^3P^o$ only, and not on those associated with the $2s^2$ 1S state. This is because in the former case, the ejected electrons can have $m = -1, 0$ or 1 , whereas in the latter they can only have $m = 0$. A description of the structure used to describe C^+ and other TDRM parameters can be found in [9, 10].

To describe the correlated electron dynamics in terms of the dynamics of individual electrons, we transform from the LS coupled basis to the uncoupled basis $|2p_{m_1}2p_{m_2}\rangle$. Since the light is linearly polarized, M is conserved. The $2s$ electron can be considered as a spectator electron for $M = 0$, so that the LS coupled $2p^2$ 1S and 1D configurations can be decomposed as follows:

$$|2p_0, 2p_0\rangle = -\sqrt{\frac{1}{3}}|2p^2 \text{ }^1S\rangle + \sqrt{\frac{2}{3}}|2p^2 \text{ }^1D\rangle \quad (1a)$$

$$|2p_1, 2p_{-1}\rangle_S = \sqrt{\frac{2}{3}}|2p^2 \ ^1S\rangle + \sqrt{\frac{1}{3}}|2p^2 \ ^1D\rangle, \quad (1b)$$

where the subscript S indicates singlet spin coupling between the $m=1$ and $m = -1$ electrons. The decomposition in eq.(1) immediately suggests that angular dynamics in the $2s2p^2$ configuration involves correlative dynamics of the two electrons: if the m -value of one electron changes, the other electron must also experience a change.

3. Results

Figure 2 shows the population of the $|2p_m, 2p_{-m}\rangle$ functions and the LS coupled states as a function of time during and after an $n=18$ cycle (7.5 fs) pump pulse. The figure shows clear evidence of Rabi oscillations between the ground and excited states during the pump pulse due to detuning. During the pump pulse, most population in the $2s2p^2$ configuration can be found in the 2D state. However, at the end of the pulse, its population has fallen back substantially. The final population in the $2s2p^2$ configuration thus consists of populations in 2S and 2D at comparable magnitudes. Consequently, after the pulse, a striking oscillation in the population of $|2p_0, 2p_0\rangle$ and $|2p_1, 2p_{-1}\rangle_S$ can be seen. Due to the energy difference between 2S and 2D , this leads to a noticeable oscillation in the $|2p_0, 2p_0\rangle$ and $|2p_1, 2p_{-1}\rangle_S$ populations after the 18 cycle pump pulse with both populations reaching a minimum value close to 0. During the pulse, oscillations between $|2p_0, 2p_0\rangle$ and $|2p_1, 2p_{-1}\rangle_S$ can be seen as well, but they do not indicate as substantial a change in the nature of the wavepacket.

Figure 3 shows the 2D momentum distributions of the ejected electron in the $k_x k_z$ plane for several pump pulse lengths. For each of the momentum distributions, the probe pulse reaches its peak intensity at a time-delay which corresponds to a minimum in the $|2p_0, 2p_0\rangle$ population and a maximum in the $|2p_1, 2p_{-1}\rangle_S$ population. The values for these time delays are given in Table 1. The momentum distributions are obtained by transforming the continuum wave functions coupled to the $1s^2 2s 2p \ ^3P^o$ excited state of C^{2+} at the end of the calculation into the momentum representation [13]. The figure shows that the ejected electrons are predominantly emitted along the laser polarization direction, except for pulse lengths of 6 and 18 cycles. Since $|m|=1$ electrons cannot be emitted along this direction, the figure shows a dominance for the emission of $m=0$ electrons. The exceptions are pulse lengths of 6 and 18 cycles, which are dominated by the emission of $|m|=1$ electrons. This is despite our choice of probing the configuration at a time when the population of $|2p_0, 2p_0\rangle$ is at a minimum and $|2p_1, 2p_{-1}\rangle_S$ at a maximum. The reason for this is that when the populations of $|2p_0, 2p_0\rangle$ and $|2p_1, 2p_{-1}\rangle_S$ are comparable, emission of an $m = 0$ electron is favoured. For most pulse lengths, population in the $2s2p^2$ configuration is dominated by the 2D state, and hence the $|2p_0, 2p_0\rangle$ and $|2p_1, 2p_{-1}\rangle_S$ have a comparable population. For pulse lengths of 6 and 18 cycles, however, population in the 2D and 2S states is comparable, and we can expect the dynamics to appear far more prominently.

Although the momentum distributions for the 6 and 18 cycle pulses in figure 3

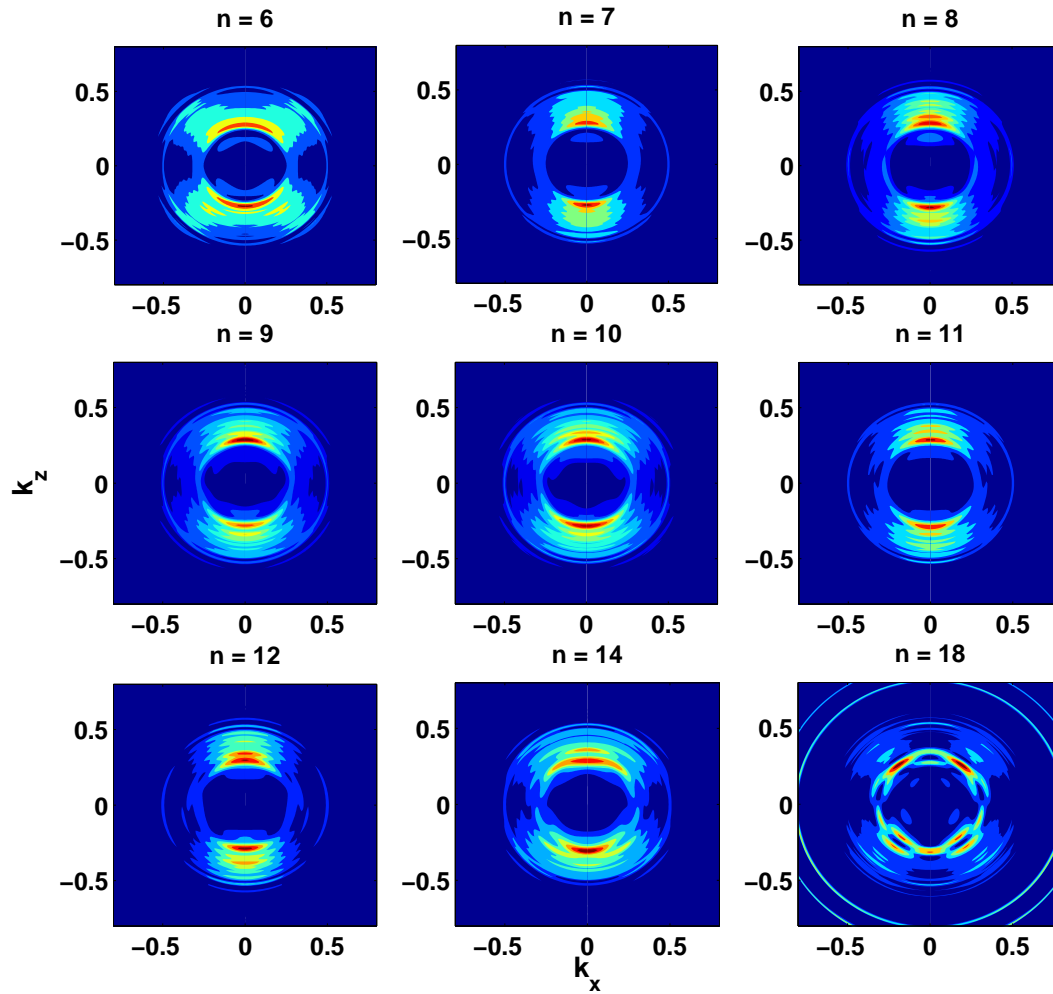


Figure 3. (Color online). Momentum distributions $|k\phi(k)|^2$ associated with the residual C^{2+} ions left in the $2s2p\ ^3P^o$ state in the $k_x k_z$ plane for the ejection of an electron from the pumped C^+ ion for varying durations of the excitation pulse. In this figure, n indicates the total number of cycles of the excitation pulse. For each distribution the probe pulse interacts with the C^+ ion when the $|2p_0, 2p_0\rangle$ population is at a minimum.

show a similar angular dependence, there are clear differences between the structure in their respective momentum distributions. The most noticeable difference can be seen at small momenta. At low momentum, figure 3 shows little interference structure for the 6-cycle pulse. On the other hand, the 18-cycle pulse shows considerable interference structure. This interference structure is, furthermore, asymmetric with respect to $k_z = 0$, which suggests interference between waves with even and odd parity. The most obvious explanation for this interference is thus interference between electrons emitted by the probe pulse, and electrons emitted during three-photon absorption from the pump pulse. The increased duration of the pump pulse should make three-photon ionization relatively more important for the 18-cycle pump pulse than for the 6-cycle pump pulse.

So far we have shown that emission of $|m| = 1$ electron occurring at a minimum in the population of $|2p_0, 2p_0\rangle$ is dominant only after a 6 cycle and 18 cycle pump pulse. We can further demonstrate that this is a good measure of the correlated dynamics occurring between the two 2p electrons after the end of the pump pulse. Figure 4 shows the momentum distributions obtained for five separate lengths of the pump pulses of varying duration, and for three delays of the probe pulse. The first delay corresponds to a minimum of the $|2p_0, 2p_0\rangle$ population, as in figure 3. The third delay corresponds to a maximum of the $|2p_0, 2p_0\rangle$ population and the second delay corresponds to the midpoint between these two delays. The values for these time delays are given in Table 1.

Table 1. Time delays (fs) between end of n -cycle pump pulse and start of probe pulse.

n	$ 2p_0, 2p_0\rangle$ min	intermediate	$ 2p_0, 2p_0\rangle$ max
6	1.89	2.25	2.68
7	1.70	-	-
8	2.64	-	-
9	2.06	2.42	2.76
10	1.81	-	-
11	1.64	-	-
12	1.50	1.91	2.30
14	1.72	-	-
15	1.43	1.86	2.27
18	1.69	2.03	2.35

Figure 4 clearly shows the dominant emission of $|m| = 1$ electrons for the 6- and 18-cycle pump pulses for delays at which the $|2p_0, 2p_0\rangle$ population is at a minimum. At the third time-delay, the probe pulse interacts with the wave-packet when the $|2p_0, 2p_0\rangle$ population is at a maximum. The dominance of the emission of $m=0$ electrons at this delay is clearly visible. This behaviour indicates that the wave-packet is undergoing a breathing motion in which it oscillates between two distinct angular distributions. The wave-packet will oscillate between these distributions after the end of the pulse with a period of 1.5 fs, determined by the energy separation between the $^2S^e$ and $^2D^e$ states. For a wave-packet prepared by the 9-, 12- or 15-cycle pump pulse, however, signs of electron dynamics are elusive. The dominance of population in the 2D state means that the breathing motion between the two angular distributions only forms a minor part of the excitation into $2p^2$.

Figure 4 thus shows that by a careful choice of the pump pulse length, it is possible to choose the nature of the excitation of the $2p^2$ configuration. For certain pulse lengths, the excitation will be dominated by a single LS-coupled state, but for other pulse lengths, the excitation will be dominated by a breathing motion between uncoupled states. Studies in this area may lead to further insight into the fundamental connection

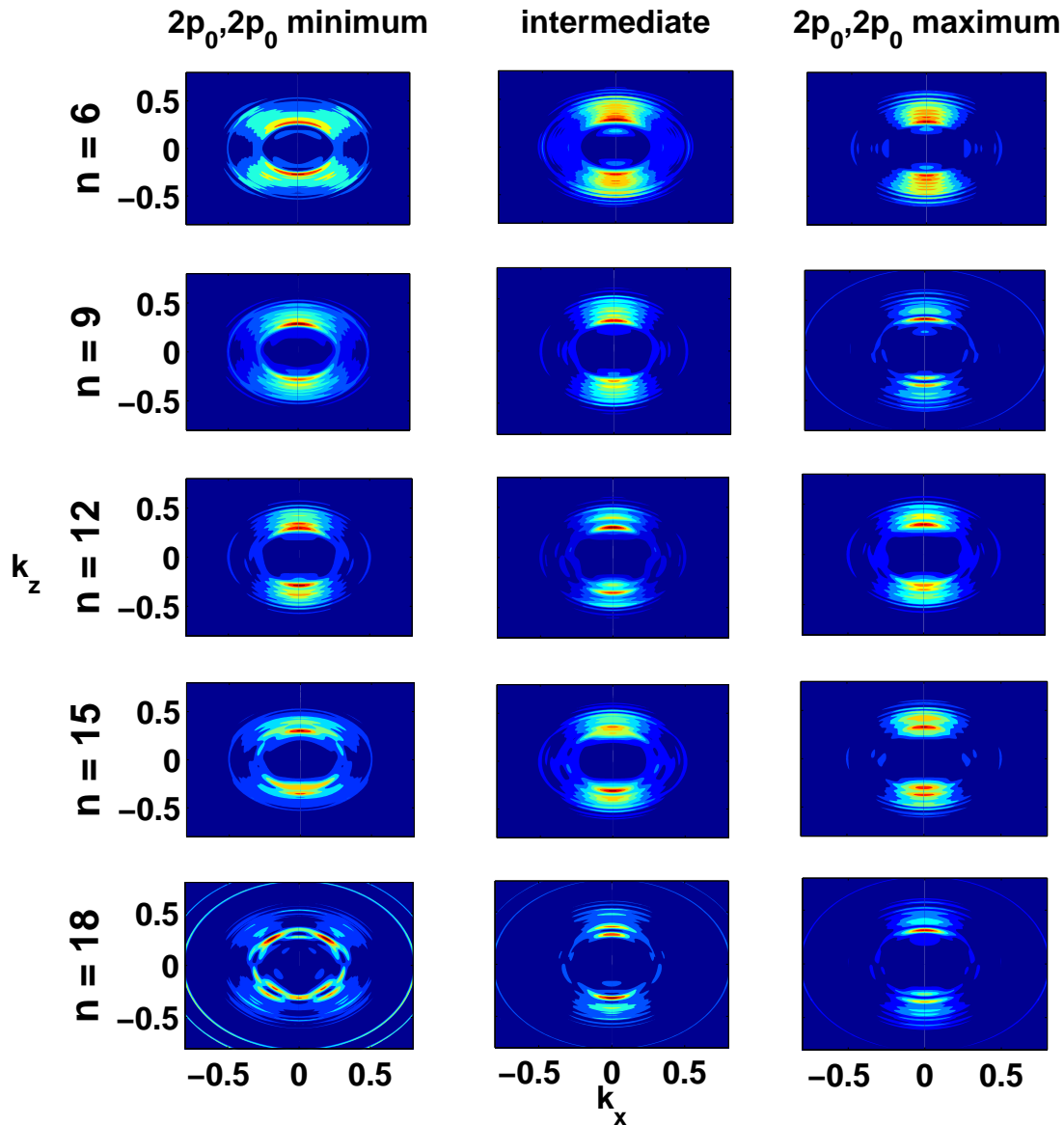


Figure 4. (Color online). Momentum distributions similar to those shown in fig. 3. The distributions have been obtained for three different pump pulse durations: $n = 6, 9, 12, 15$ and 18 cycles. For each pump pulse the probe pulse ionizes the pumped system at three increasing time delays, where 'intermediate' indicates a delay at which $|2p_0, 2p_0\rangle$ is half way between its minimum and maximum population.

between atomic structure and correlated multi-electron dynamics.

The scheme presented here demonstrates the possibility of influencing the “dynamical” alignment of a multielectron wave-packet by varying the duration of single laser pulse. However, the use of a single pump pulse has significant drawbacks. For example, it is difficult to transfer significant population into the 2D and 2S states. However, this problem could be alleviated by the use of multiple pump lasers. For example, an XUV pulse could be used to resonantly populate the $2s2p^2$ 2D state with a second long wavelength pulse used to couple the 2D and 2S states via a 2-photon

transition. The long wavelength pulse could be tuned to this 2-photon transition, thereby reducing the effect of detuning seen in the present study. The amount of population pumped into the excited states could also be controlled by the long wavelength laser parameters.

4. Conclusion

In conclusion, we have applied time-dependent R-matrix theory to illustrate a technique that may provide the ability to steer multielectron wave-packets into a specific field-free evolution. In the present application to the $2s2p^2$ configuration of C^+ , we have shown that the field-free angular dynamics of the two-electron wave-packet is dominated by a breathing motion between two $2p$ electrons with $m=0$ and two $2p$ electrons with $|m|=1$ for an excitation pulse of 10 eV with pulse lengths of 6 and 18 cycles, whereas for pulse lengths inbetween the two-electron wavepacket is dominated by the 2D state. Although the present single pump pulse scheme allows a choice of dynamics for the two-electron wave-packet, more elaborate pulse schemes are required to transfer significant population into such dynamics. It would also be interesting to extend this study to more complex configurations to obtain additional insight into the influence of electron-electron interaction on correlated multi-electron dynamics.

5. Acknowledgments

ML acknowledges support through Grant No. EP/E000223/1 from the UK EPSRC.

References

- [1] M. Uiberacker *et al.* Nature **446**, 627, (2007)
- [2] O. Smirnova *et al.* Nature **460**, 972, (2009)
- [3] D. V. Vyalikh *et al.* Phys. Rev. Lett. **102**, 098101, (2009)
- [4] M. Stockman *et al.* Nat. Photonics **1**, 539, (2007)
- [5] G. Sansone *et al.* Science **314**, 443, (2006)
- [6] D. Shafir *et al.* Nature Phys. **5**, 412, (2009)
- [7] A. L. Cavalieri *et al.* Nature **449**, 1029, (2007)
- [8] T. Morishita *et al.* Phys. Rev. Lett. **98**, 083003, (2007)
- [9] M. A. Lysaght, P. G. Burke and H. W. van der Hart Phys. Rev. Lett. **102**, 193001, (2009)
- [10] M. A. Lysaght, S. Hutchinson and H. W. van der Hart New J. Phys. **11**, 093014, (2009)
- [11] C. Froese Fischer *et al.* Computational Atomic Structure: An MCHF approach, chp 2.2.2, IOP, Bristol (1997)
- [12] Burke P G and Burke V M 1997 J. Phys. B: At. Mol. Opt. Phys. **30**, L383
- [13] M. A. Lysaght, H. W. van der Hart and P. G. Burke Phys. Rev. A **79**, 053411, (2009)
- [14] P. G. Burke and K. A. Berrington, Atomic and Molecular Processes: an R-matrix Approach, IOP, Bristol (1993)